Nanotechnology

PAPER

Efficient metallic nanowire welding using the Eddy current method

IOP Publishing Nanotechnology
Nanotechnology 30 (2019) 065708 (10pp) https://doi.org/10.1088/1361-6528/aaf13d

Efficient metallic nanowire welding using the Eddy current method

Ji Soo Oh[1], Jong Sik Oh[1], Tae Hyung Kim[1] and Geun Young Yeom[1,2]

[1] School of Advanced Materials Science and Engineering, Sungkyunkwan University, Suwon 16419, Republic of Korea
[2] SKKU Advanced Institute of Nano Technology (SAINT), Sungkyunkwan University, Suwon 16419, Republic of Korea

E-mail: gyyeom@skku.edu

Received 18 September 2018, revised 8 November 2018
Accepted for publication 15 November 2018
Published 13 December 2018

Abstract

In this study, metallic nanowires (M-NWs) such as silver nanowires (AgNWs) and copper nanowires (CuNWs) were welded only at junctions resistively by a novel method using an indirect Eddy current through an inductive power transfer. By applying an inductive power of 45 kHz alternating current power indirectly for 6 s to the M-NW network deposited on polymer substrates, a decrease of sheet resistance up to ~67.9% for AgNWs and ~49.9% for CuNWs could be obtained without changing the optical transmittance. For AgNWs, after the welding a decrease of surface roughness could also be observed from 44.5 nm to 26.3 nm, which is similar to the height of a single layer AgNW (22.2 nm) for a bilayer junction. For AgNWs coated on a transparent flexible substrate, after the cyclic bending of 10 000 times, no change of resistance ($\Delta R/R0$) of the AgNWs after the welding was observed and the welded AgNWs were not easily peeled off from the substrate. It is believed that this novel welding method can be applied not only to all kinds of M-NWs on various flexible low-temperature polymer substrates, but also to large areas at a short time and at low cost.

Supplementary material for this article is available online

Keywords: nanowire, nanowelding, Eddy current, inductive coil system

(Some figures may appear in colour only in the online journal)

1. Introduction

The most commonly used transparent conductor is indium tin oxide (ITO). However, ITO is not suitable for next-generation flexible electronic devices due to its brittleness and the scarcity of indium, and also the requirement of high-temperature annealing after vacuum deposition [1, 2]. Therefore, various alternative conducting materials to ITO such as carbon nanotubes [3, 4], graphene [2, 5, 6], conducting polymers [7, 8], and metallic nanowires (M-NWs) [9–12] have been extensively investigated. Among these, M-NWs such as silver nanowires (AgNWs) and copper nanowires (CuNWs) have been identified as leading alternatives because they have the lowest sheet resistance at a given transparency [10, 13–21]. M-NWs can not only provide a similar sheet resistance and transparency to ITO but also are highly flexible, low cost, and solution-processible [13, 22–28]. However, despite all the advantages of M-NW electrodes, there are some issues to be resolved; one of these is the surface roughness. For the M-NW connection, junctions are required, where several nanowires (NWs) are stacked on top of one another. The inherently rough surfaces of the NW networks caused by the NW thickness itself at the junctions can cause increased haziness in addition to high surface roughness. Other important issues include the lack of long-term stability and the low adhesion to the substrate due to weak adhesive forces between the substrate and NWs. These problems such as high haziness, high surface roughness, lack of long-term stability, and low adhesion can be partially removed by welding processes such as thermal [19, 29–31], mechanical [32–34],

electrical [35–37], plasmonic [14, 38–40], and electrochemical treatment [41–44], or through integration with other materials [45–48]. Recently, the wet welding method utilizing moisture was also introduced [49]. While these welding methods have their own advantages, they tend to be difficult to apply to low-temperature polymer substrates; in addition, the substrate and the active layers on the substrate can be physically damaged. Furthermore, they can require several steps including the application of chemicals, washing, drying, etc. It is reported that electrical and plasmonic methods can provide heating of the NW junction only; these methods are therefore useful for NW welding without physically/chemically affecting the substrates and without decreasing the optical transmittance [14, 35–40, 50].

To flow electrical current into the M-NWs without touching the NWs, a welding process using an indirect Eddy current method is herein introduced. The indirect Eddy current method is a simple method of fusing M-NW junctions only resistively using an Eddy current flow induced by inductive power. Generally, heating by induction is clean, efficient, cost-effective, and a repeatable method of materials heating available in industry [51]. Similar to previously investigated plasmonic and electrical methods, this nanowelding method accomplished the welding without decreasing the optical transmittance, without increasing the substrate temperature, without deforming the wire structure, and most particularly, did this in a very short welding time (within seconds). It is believed that this approach has the potential to be applied to all M-NWs including AgNWs and CuNWs on a large scale substrate efficiently.

2. Experimental

2.1. NW

Commercially available AgNWs (NANOPYXIS, with a length of 22 ± 5 um and diameter of 25 ± 3 nm) and CuNWs (Novarials, with a length of 50–200 um and diameter of 50–100 nm) were used in this experiment. These AgNWs and CuNWs were then diluted with 10 ml of isopropyl alcohol (IPA) to 0.05 wt% to form M-NW solutions.

2.2. Fabrication

A variety of substrates including a glass substrate, PEN (polyethylene naphthalate) substrate, etc. were used to spray M-NWs; before spraying the M-NW solution, the substrates were cleaned in acetone, alcohol, and deionized water (DIW) by sonication. M-NWs were spray coated using a spray equipment (air spray gun; SPAR GP-35) capable of uniform coating M-NWs by using a heated X-Y stage as shown in figure 1(a). The M-NW solution was sprayed with 15 psi of N_2 gas while heating the stage to about 50 °C in order to easily remove the solvent. Through the coating, a uniform NW film was obtained and, for AgNW films, an initial sheet resistance of 100 Ω/sq was obtained on various substrates.

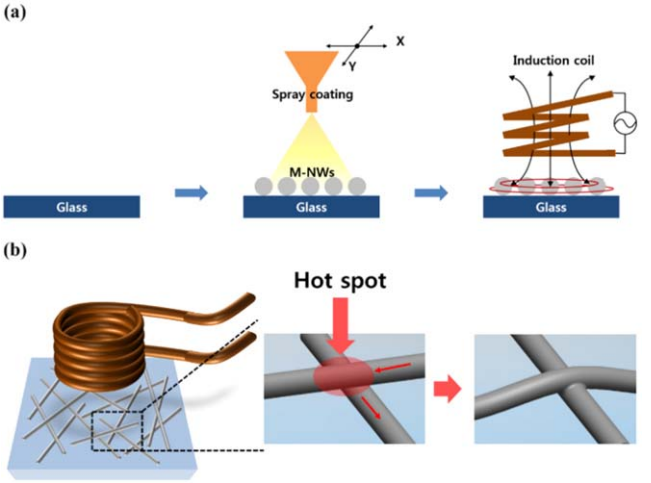

Figure 1. (a) Spray coating with a heated X-Y stage used in the experiment for uniform coating of M-NWs. (b) Schematic illustration of coil heating and generation of Eddy current on the substrate.

The CuNW films were also fabricated on various substrates with its initial sheet resistance of 150 Ω/sq.

2.3. Welding

The M-NW coated substrates were welded by inductive heating as shown in figure 1(b) and the welding was carried out in a nitrogen atmosphere to prevent the oxidation of M-NWs. The components of the welding system used in this study consisted of a high-frequency power supply, a seven-turn inductive coil, and a welding chamber with the coil connected. The frequency of the inductive welding system used in the experiment was 45 kHz, and the inductive coil diameter/thickness were 45 mm/5 mm. The distance between the inductive coil and the substrates was kept at 2.5 cm. For the welding, the inductive power (current condition; $5 \sim 25$ A) and the welding time (from 1 to 10 s) were varied to observe the resistance change of the M-NW film.

2.4. Characterization

Welding characteristics of the M-NWs were observed using field emission scanning electron microscopy (FE-SEM; Hitachi S-4700). The changes of the NW morphology were observed using atomic force microscopy (AFM; INOVA). Optical transmittance was observed using optical micrographs and was measured using ultraviolet-visible spectroscopy (UV-3600; Shimadzu). The sheet resistance was measured using a four-point probe method (Keithley 2000; Keithley). The mechanical integrity of the M-NW film on the substrate was measured using a lab-made bending test system bended to a radius of curvature of 5 mm. The degree of adhesion strength of the M-NW film on substrates was roughly estimated using the peel-off method using a 3 M tape. The composition of CuNWs after the long welding was analyzed using energy dispersive spectroscopy (EDS; HORIBA EMAX-250) to investigate the possible oxidation of the CuNWs' surface during the welding.

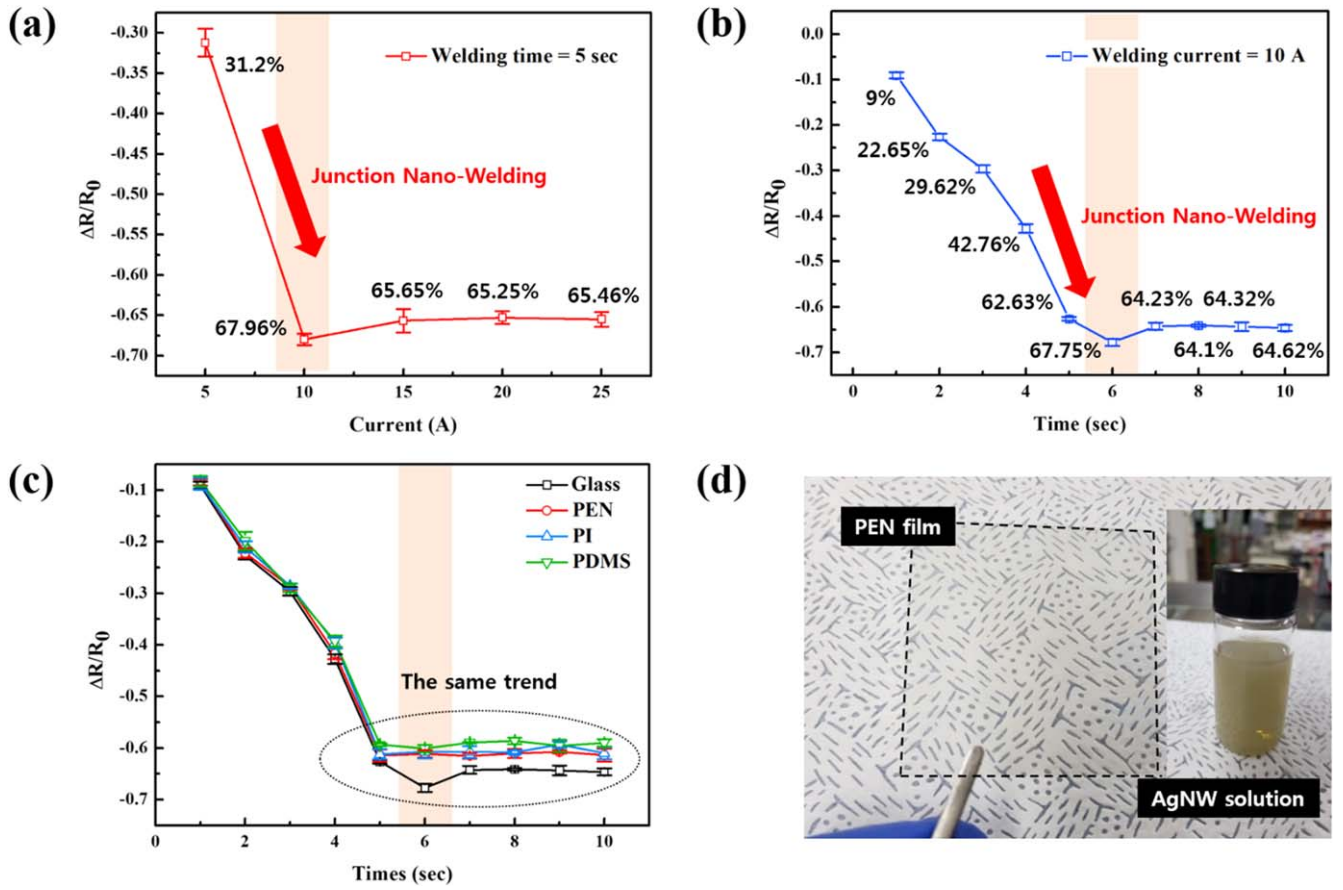

Figure 2. (a) Change of AgNW sheet resistance measured as a function of the inductive coil current while keeping the welding time at 5 s. (b) Change of sheet resistance measured as a function of the welding time while keeping the inductive heating current at 10 A. (c) Change of sheet resistance for different substrates such as PEN, PI, and PDMS while keeping the inductive heating current at 10 A. (d) An image of welded AgNWs on the PEN substrate and the AgNW solution used in the experiment.

3. Results and discussion

3.1. Welding of M-NWs by the Eddy current method

M-NWs were spin-coated on various substrates and the induction coil was located 2.5 cm above the M-NW coated substrate, as shown in figure 1(a). The induction frequency used in the experiment was 45 kHz (generally in the range of 7 ∼ 500 kHz and the induction heating was generally used for heat treatment, brazing, and melting of metals [52]) and the current to the induction coil was varied from 0 to 50 A.

As shown in figure 1(a), when a radio frequency (RF) power is delivered to the induction coil, an alternating magnetic field is generated and, as the alternating magnetic field propagates through conductive materials, an Eddy current is generated within the thin skin depth of the materials, which induces Joule heating [51–57] (generally, 'Eddy current' refers to the multiple current loops induced on the solid/bulk conductor surface perpendicular to the alternating magnetic field, while for a current induced on a coil-like loop, it is just referred to as 'induced current'. In the case of a AgNW network, even though the NWs form a coil-like loop, they also form a sheet of conductor as a network on the substrate surface; therefore, the current induced on the AgNW is closer to an 'Eddy current' which forms multiple induced current loops on the surface). In the case of M-NWs, as shown in figure 1(b), the Eddy current flows to the NW network and a hot spot is generated at the NW junctions due to the high resistance at the NW junction and the NW junctions are melted locally without heating the rest of the NW areas (a more detailed figure on the Joule heating at the NW junction by the induced Eddy current is shown in figure S1 of the supporting information, which is available online at stacks.iop.org/NANO/30/065708/mmedia).

3.2. Welding of AgNWs

With the AgNWs sprayed on the glass substrate to have an initial sheet resistance of ∼100 Ω/sq, the AgNWs were welded by the Eddy current method using induction heating while varying the induction coil current (0∼25 A) and welding time (1∼10 s). The resistances of the M-NWs before and after the welding were measured by a four-point probe. Figure 2(a) shows the change of AgNW sheet resistance measured as a function of the inductive coil current while keeping the welding time at 5 s. As shown, with the increase of the coil current from 0 to 10 A, the sheet resistance was decreased significantly, and the change of sheet resistance ($\Delta R/R_0$) was ∼31.2% at 5 A and ∼67.96% (which changes from 106.64 to ∼34.16 Ω/sq) at 10 A. The further increase of

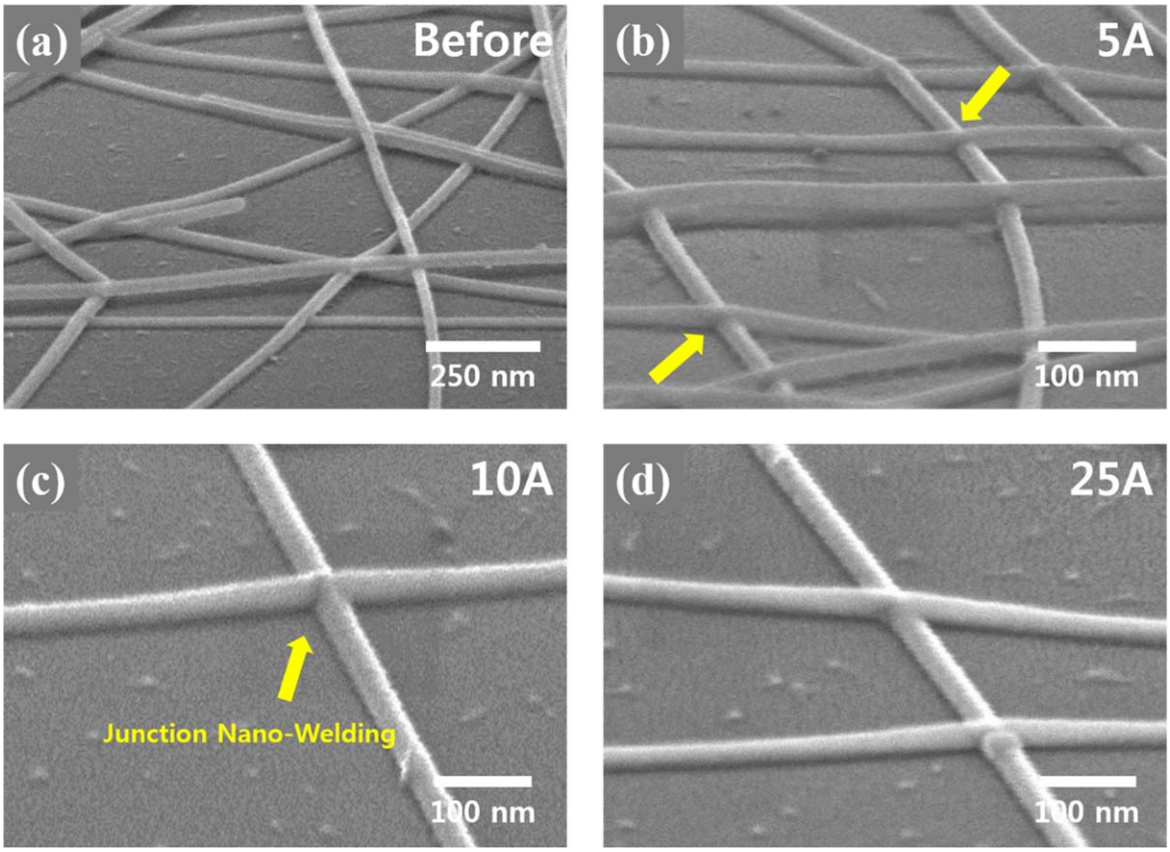

Figure 3. FE-SEM images of AgNWs (a) before welding and after welding with (b) 5 A, (c) 10 A, and (d) 25 A for 6 s.

inductive coil current to 25 A did not much change the sheet resistance. While keeping the inductive coil current at 10 A, the welding time was increased from 1 to 10 s and the change of sheet resistance ($\Delta R/R_0$) was measured as a function of the welding time; the results are shown in figure 2(b). The sheet resistance was decreased with the increase of the welding time up to ~6 s but the further increase of welding time to 10 s did not change the resistance. At 6 s of welding time, the change of sheet resistance was the lowest at ~67.75% (the sheet resistance changed from 109.12 to 35.2 Ω/sq). In figure 2(c), the AgNWs were sprayed on various substrates such as PEN, PI (polyimide), and PDMS (polydimethylsiloxane) in addition to the glass substrate, and the change of sheet resistance was measured as a function of welding time for the welding condition outlined in figure 2(b). As shown in figure 2(c), the change of sheet resistance for different substrates such as PEN, PI, and PDMS was similar to that for the glass substrate and the sheet resistance at ~5 s showed a 60%~64% decrease from the un-welded AgNWs regardless of the substrates. Therefore, by using the Eddy current method, the welding of AgNWs could be achieved regardless of substrates (in case the substrate is an insulator which does not induce an Eddy current). Figure 2(d) shows the image of welded AgNWs on the PEN substrate using the AgNW solution in the inset. Therefore, the AgNW network with an optical transmittance higher than 90% and sheet resistance lower than 40 Ω/sq could be obtained by welding for 6 s using the Eddy current method; this is the shortest welding time among the AgNW welding methods which obtained an optical transmittance higher than 90% and sheet resistance lower than 40 Ohm/sq, as shown in table S1 of the supporting information.

To understand the change of sheet resistance observed in figure 2, the AgNW networks before and after welding were observed using FE-SEM for the condition shown in figure 2(b). A SEM image of the AgNW contacts before the welding treatment is shown in figure 3(a), and a sharp interface between the two top and bottom NWs in contact (NW junction) is clearly visible. Figures 3(b)–(d) show SEM images of the AgNWs after the welding treatment for 6 s with different inductive coil currents of 5, 10, and 25 A respectively. As shown in figures 3(b) and (c), as the inductive coil current is increased to 5 and 10 A, the NW junction part was fused further. In order to confirm that the NW junction of the AgNW is clearly fused, a transmission electron microscope measurement was performed. As can be seen from the supporting information in figure S2, the junction was reliably welded.

However, as shown in figure 3(d), when the inductive heating current was increased further to 25 A, the AgNW junction morphologies remained similar to those seen at 10 A, indicating the stabilization of the AgNW junction. The Eddy current method generates heat mostly at the junction part of a NW network by forming a hot spot at the junction; this is due to the highest resistance being found at the junction. Therefore, after the complete welding of the junction, no further

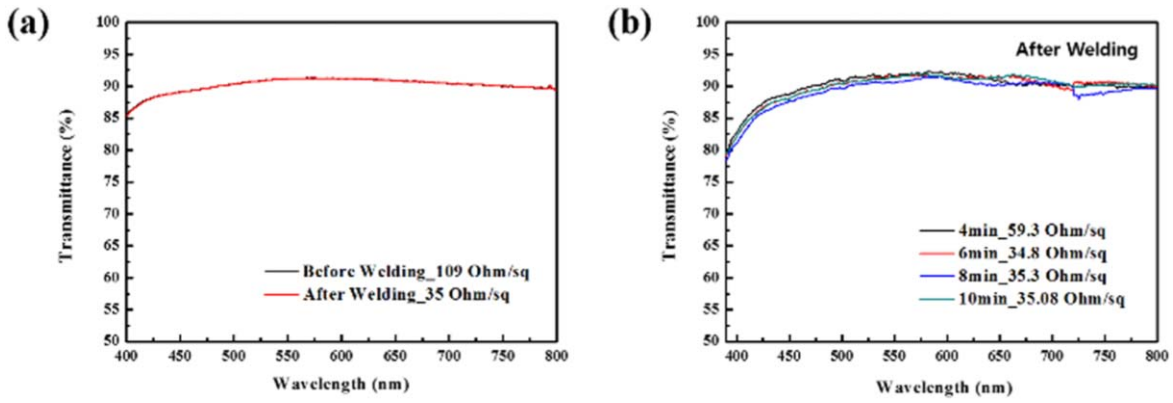

Figure 4. (a) Optical transmittance of the glass substrate coated with AgNWs before and after the welding at the optimized condition (10 A, 6 s). (b) Optical transmittance of the glass substrate coated with AgNWs after the welding from 4 to 10 min which is 100 times longer than the optimized welding time.

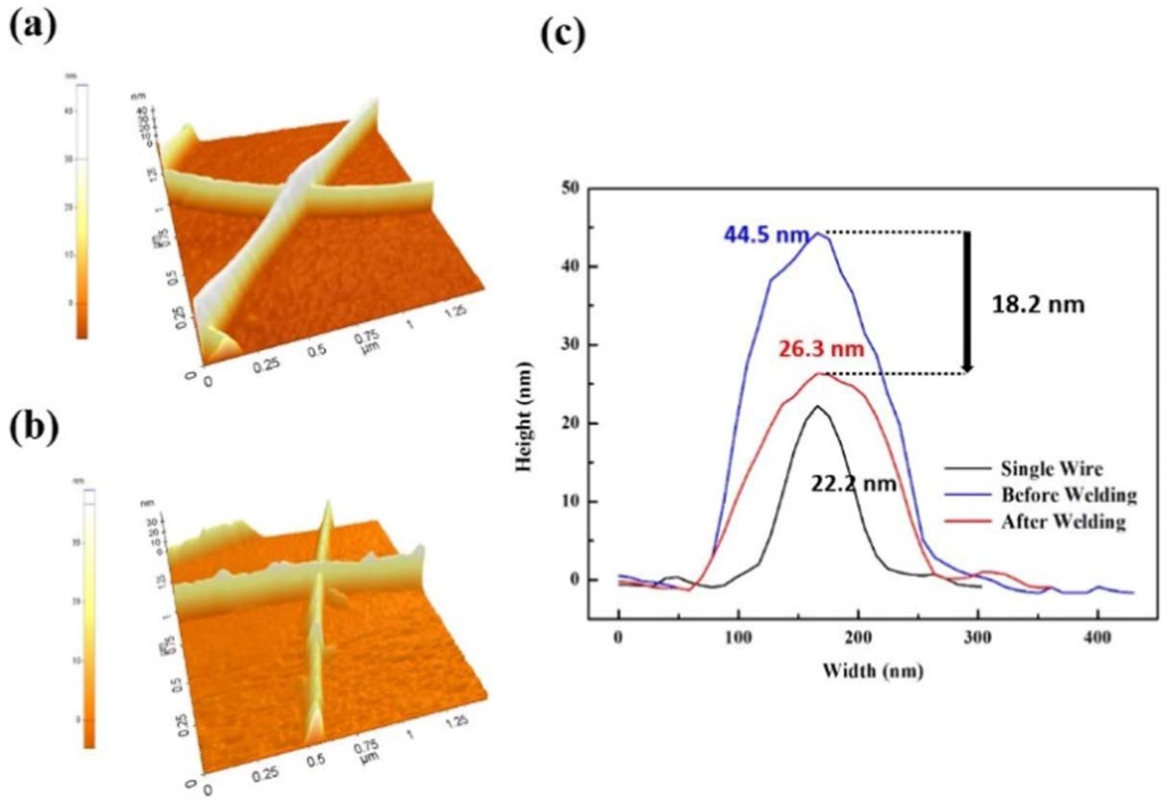

Figure 5. AFM 2D surface roughness of the AgNW junction (a) before and (b) after welding at the optimized condition (10 A and 6 s). (c) Line scan data of the single AgNW and the AgNW junction before and after the welding.

deformation of the AgNW junction was observed for the higher inductive heating current (up to 25 A at 6 s) or for a longer welding time (up to 10 min at 10 A) than the optimized welding condition (10 A and 6 s) due to the removal of the hot spot at the junction. Therefore, it is found that if the inductive coil current is not too high, complete fusion of a AgNW junction can be achieved on a large current window and wide welding time window.

Figure 4(a) shows the optical transmittance of the glass substrate coated with AgNWs before and after the welding at the optimized condition (10 A, 6 s). As shown in figure 4(a), almost no change in the optical transmittance (at 550 nm, the optical transmittance was 91.09% before the welding while that after the welding was 91.09%) was observed. When the welding time was significantly increased to 10 min which is 100 times longer than the optimized welding time at 10 A of the inductive heating current, as shown in figure 4(b), no change of optical transmittance was observed.

The surface roughness of the AgNW before and after welding at the optimized condition (10 A and 6 s) was investigated using AFM and the results are shown in figures 5(a) and (b) for the area scan data of the AgNW before

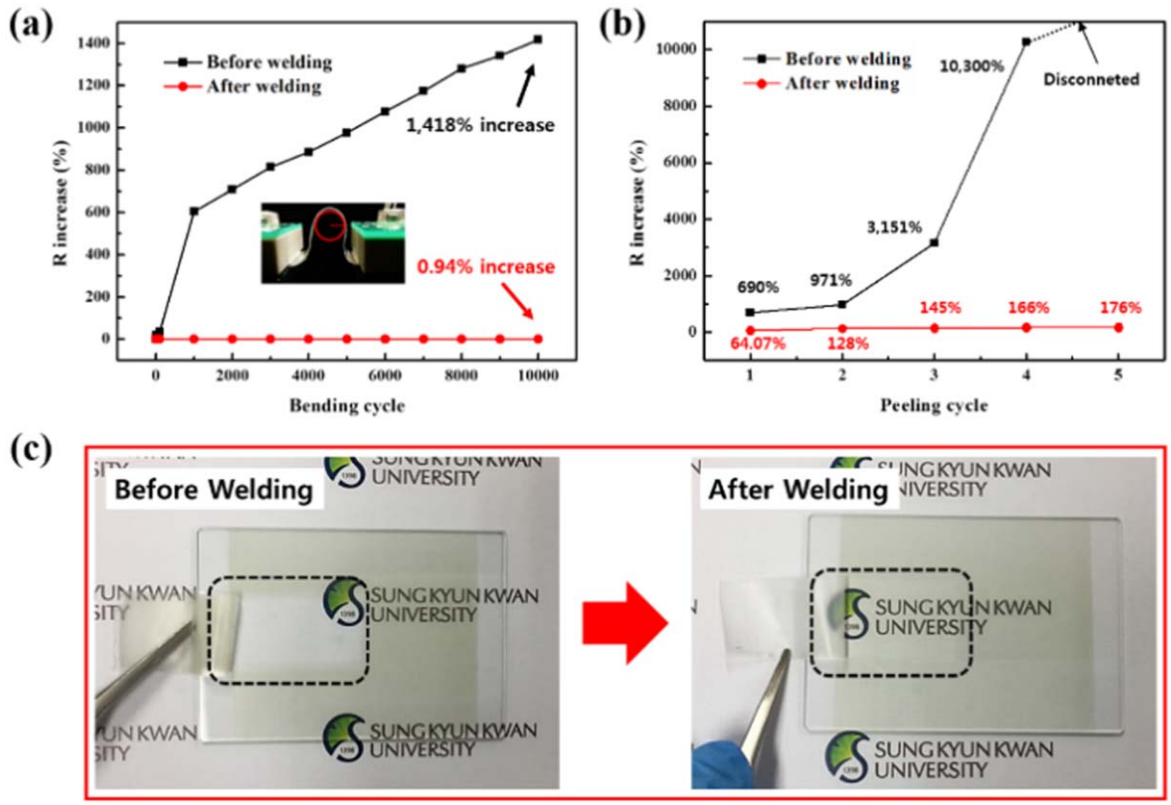

Figure 6. (a) Change of sheet resistance of the AgNWs on PEN substrates before and after welding measured as a function of bending cycles. The inset is a photograph of the bending test used in the experiment and, as shown, the bending radius of the flexible substrate was decreased to 5 mm and the bending test was carried out up to 10 000 cycles. (b) Change of the sheet resistance of the AgNWs on glass substrates after peeling off with a 3 M tape on the AgNW film up to five times. (c) Optical micrographs of the AgNWs coated on the glass substrates after peeling off AgNW before and after welding with 3 M tape, respectively. After welding, the adhesion of AgNWs to the substrate was significantly improved.

and after the welding, respectively, and in figure 5(c) for line scan data of the single AgNW and the AgNW junction before and after the welding. As shown in figures 5(a) and (b), after the welding, the surface roughness was decreased due to the fusion of two AgNWs at the junction. As shown in figure 5(c), before the welding, the height of the AgNW junction was ∼44.5 nm while the height of the single AgNW was ∼22.2 nm. Therefore, before the welding, a single AgNW was physically resting on the top of another single AgNW at the AgNW junction. However, after the welding, the height of the AgNW junction decreased to ∼26.3 nm indicating almost complete fusing of two AgNWs at the junction, as shown in figure 3(d). Therefore, after the welding, the surface roughness of the AgNW network was significantly decreased.

For the application of AgNWs as electrodes for various devices including flexible devices, the durability of the AgNW electrodes coated on the substrates was investigated by performing a bending test and peeling test. The resistances of AgNWs before and after welding were 104 Ω/sq and 40.7 Ω/sq, respectively. For the bending test before and after the welding, a AgNW spray coated on a 70 mm × 15 mm PEN substrate was used. Figure 6(a) shows the change of sheet resistance of the PEN substrate with the AgNWs before and after the welding measured as a function of bending cycles, and the inset image shows a photograph of the bending test used in the experiment; as shown, the bending radius of the flexible substrate was decreased to 5 mm and the bending test was carried out up to 10 000 cycles. As shown in figure 6(a), the resistance of the PEN substrate with AgNW before the welding increased with increasing bending cycles and showed a ∼1418% increase after 10 000 cycles, possibly due to the separation of the junction during the bending. However, in the case of the substrate with AgNW after the welding (a ∼0.94% increase after 10 000 cycles, as shown in figure S3(a) of the supporting information), the resistance remained similar even after 10 000 cycles of bending; this was due to the nonseparation of the junction by the bending test because it was completely fused.

The adhesion force of the AgNWs to the substrate was roughly investigated by a peel test using 3 M scotch tape. The AgNW spray coated on the glass substrate before and after the welding was taped with the 3 M tape and the change of the sheet resistance of the AgNW after peel off with the 3 M tape on AgNW film up to five times was measured and the results are shown in figure 6(b). To measure the change of resistance more accurately and to observe the AgNW on the substrate after the peel-off test more clearly, the AgNWs with the lower sheet resistance of ∼60 Ω/sq before the welding and ∼20 Ω/sq after the welding were used. As shown in figure 6(b), the sheet

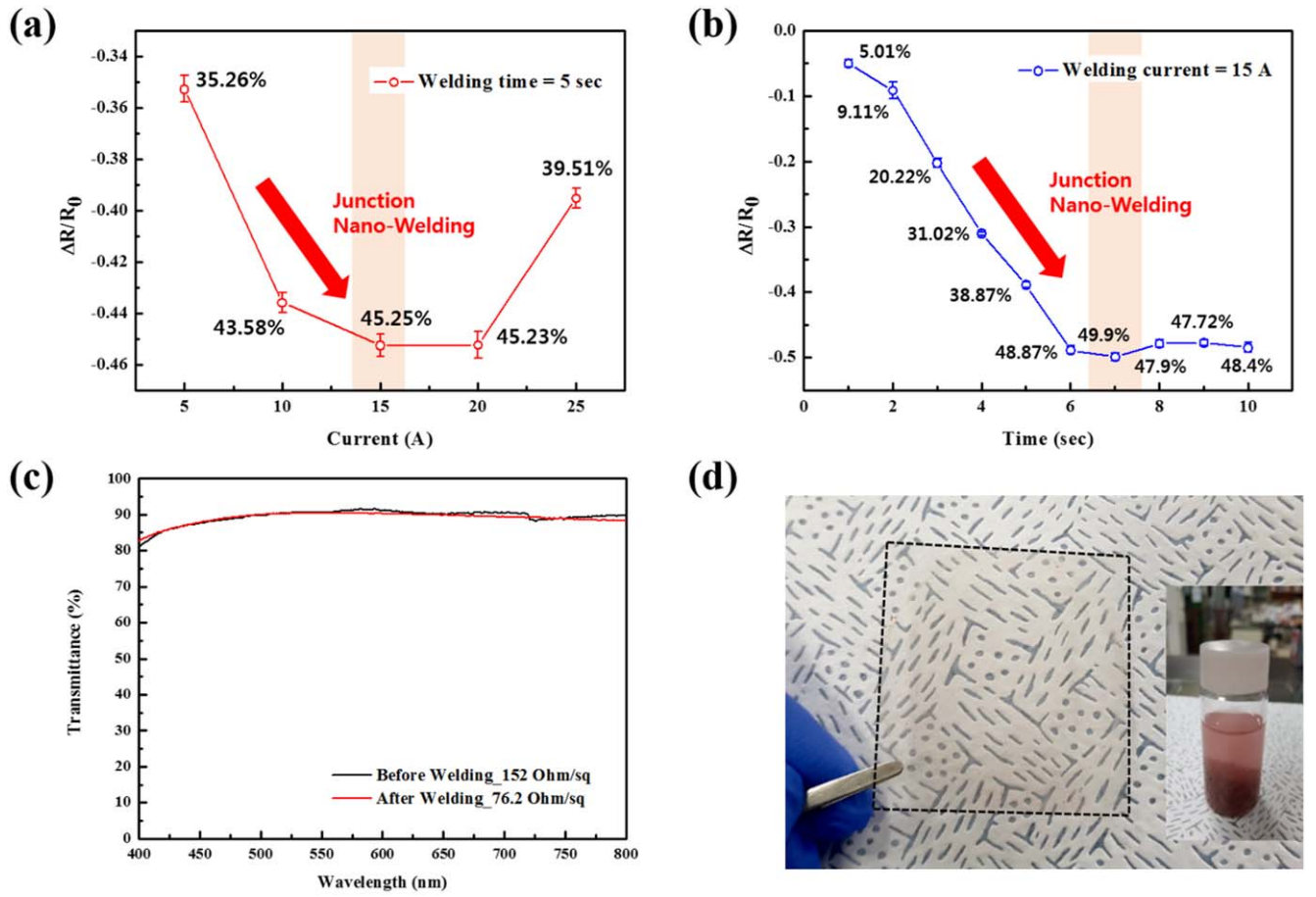

Figure 7. Change of sheet resistance of CuNWs with increasing (a) the inductive heating current (at 5 s) and (b) the welding time (at 15 A). (c) Optical transmittance of CuNW coated glass substrate before and after welding for an optimized condition of CuNW welding (15 A, 6 s). (d) An image of welded CuNWs on a PEN substrate and the CuNW solution used in the experiment.

resistance of the AgNW coated on the glass substrate before the welding was increased significantly with increasing the number of peel-off cycles by showing ∼104 times increase of sheet resistance after four cycles of peel-off test and no resistance was measured when proceeding with the peel-off test five times. It is possibly due to the no adhesion force between separate AgNWs on the substrate. However, in the case of the AgNW after the welding, the sheet resistance was increased slowly by showing a ∼2.8 times increase after five cycles of the peel-off test (figure S3(b) shows the detailed resistance change for welded AgNWs) possibly due to the connection of separate AgNWs by fusion at the junction. Figure 6(c) shows optical micrographs of the AgNWs coated on the glass substrates after the first cycle peeling off AgNW before and after welding with the 3 M tape. As shown, for the AgNW before the welding, the AgNWs were removed from the substrate with the tape while for the AgNW after the welding, no significant removal of AgNW from the substrate could be observed. The improvement of mechanical durability during the bending, peeling, and adhesion tests observed in our experiment after the welding are related to the enhanced binding of AgNW with the substrates in addition to complete binding of AgNW junctions [9, 24, 33, 44, 50].

3.3. Welding of CuNWs

Welding using the Eddy current method can be applied not only to AgNWs but also other M-NWs. To investigate the possibility of welding other M-NWs by the Eddy current method, CuNWs which are more easily oxidized and thicker than AgNW were also welded by the Eddy current method. The CuNWs were coated on the glass substrate and the initial sheet resistance of the CuNWs coated on the glass substrate before the welding was maintained at 150 Ω/sq. Figures 7(a) and (b) show the change of sheet resistance of CuNWs with increasing the inductive coil current (at 5 s) and the welding time (at 15 A), respectively. As shown in figure 7(a), when the inductive coil current was increased while keeping the welding time at 5 s, the sheet resistance of CuNW deposited on the glass substrate was decreased with increasing the current up to 15 A from ∼150 Ω/sq to ∼83.2 Ω/sq (ΔR/Ro ∼ 45.25%) and the sheet resistance remained similar up to 20 A. However, when the inductive coil current was further increased to 25 A, the sheet resistance was increased. The welding time was varied while keeping the inductive coil current at 15 A, and as shown in figure 7(b), the sheet resistance was decreased until 6 s from ∼150 Ω/sq to ∼76.1 Ω/sq (ΔR/Ro ∼ 49.9%) and the further increase of welding time did not change the sheet resistance until 10 s. The

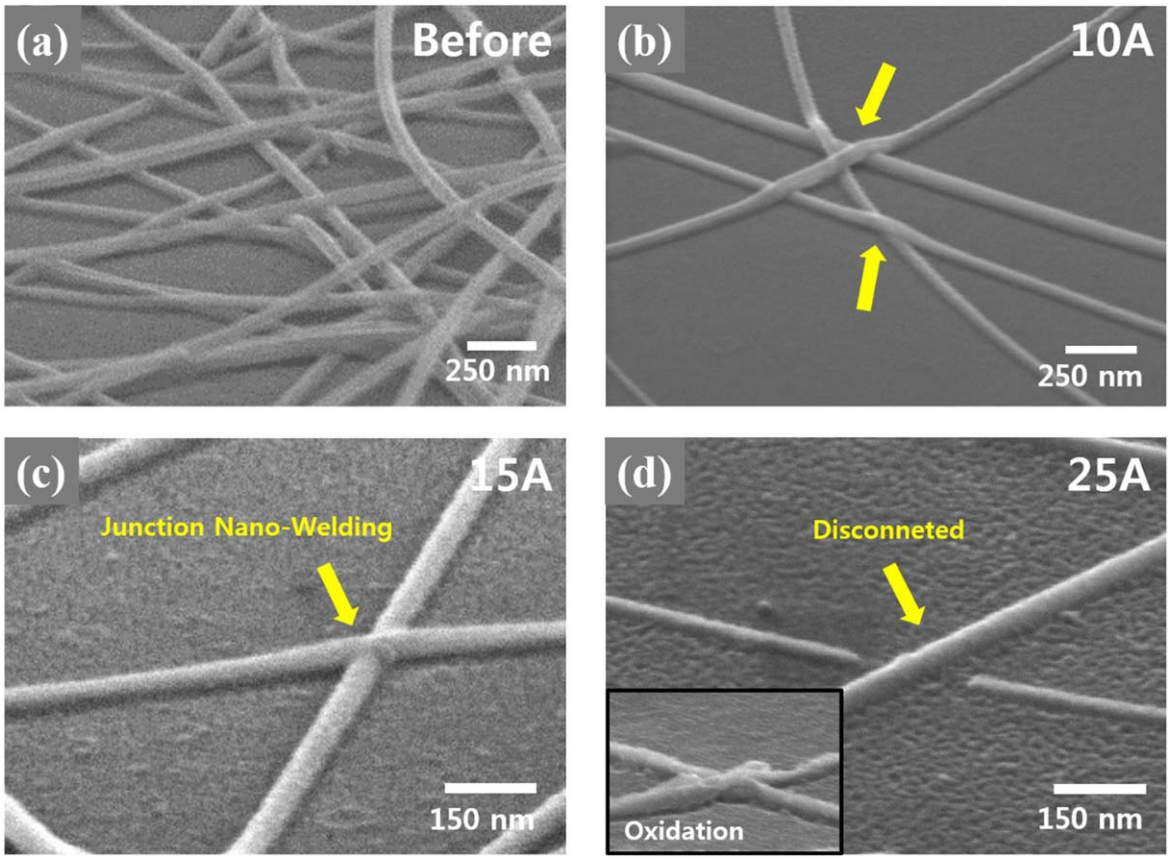

Figure 8. SEM images of the CuNW contacts (a) before the welding treatment and (b) after the welding treatment for 10 A, (c) 15 A, and (d) 25 A for 5 s. The inset image in (d) shows the junction area for (d).

optical transmittance of the CuNW coated glass substrate before and after welding for an optimized condition of CuNW welding (15 A, 6 s) was investigated and the results are shown in figure 7(c). As shown, after the welding, no noticeable change of optical transmittance (from 90.5% before the welding to 90.4% after the welding at 550 nm) could be observed. Therefore, even though the decreased percentage of the sheet resistance after the welding was smaller, similar welding characteristics to that of the AgNW could be observed.

Figure 8 shows SEM images of the CuNW junction (a) before the welding treatment and after the welding treatment for (b) 10 A, (c) 15 A, and (d) 25 A at 5 s. As shown in figure 8(a), before the welding of CuNWs, a sharp interface at the CuNW junction is seen. After the welding, the fusion of CuNWs at the junction is clearly seen, as similar to the AgNW welding, however, no complete fusion of the junction —as shown in figure 3(c)—could be observed. The smaller decrease of sheet resistance after the welding for the CuNW compared to AgNW (~67.96% for AgNWs versus ~49.9% for CuNWs) appears to be related to the less complete fusion of the CuNW junction due to the oxidized CuNW surface before the welding and the oxidation of the CuNW surface during the welding, possibly due to some oxygen partial pressure in the N_2 environment (our N_2 environment of the welding chamber is similar to the N_2 glove box, so some oxygen partial pressure exists in the system). For the inductive coil current of 25 A, the CuNW junction was finally disconnected, possibly due to the oxidation of the junction as shown in the inset (after the welding at 25 A for 5 s, some junction areas showed the oxidized junction, as shown in the inset; the oxidation of the CuNW junction for the welding condition of 25 A for 5 s could be identified by analyzing the composition of the CuNW junction before and after the welding at 25 A for 5 s, as shown in figure S4(a) (CuNWs typically oxidized as in the SEM image of figure S4(b).) Even though a nitrogen environment was used, the CuNW junctions were oxidized by residual oxygen due to the rapid oxidation characteristics of CuNWs [15, 16, 58, 59]). Even though the operating windows for the welding condition are smaller than AgNW welding, the welding of the CuNW junction without decreasing the optical transmittance could be observed by using the Eddy current method similar to AgNW welding.

4. Conclusions

A novel welding method for M-NWs—which are widely investigated as next-generation transparent and flexible conductive electrodes—using an indirect Eddy current through an inductive heating power has been investigated, and the effect of welding by the Eddy current method on the sheet resistance, surface roughness, and optical transmittance was investigated for M-NWs such as AgNWs and CuNWs. The

welding using the Eddy current generates hot spots only at the M-NW junctions due to the higher contact resistance at the junction compared to the M-NW itself, therefore, only the M-NW junctions can be welded without heating the M-NW itself and the dielectric substrates such as polymer substrates and glass substrates. The results showed that through welding by the Eddy current method, a sheet resistance decrease of ~67.96% for AgNWs and ~49.9% for CuNWs could be observed without changing the optical transmittance and without heating the dielectric substrates. In the case of AgNWs, due to the complete fusion at the junction, the surface roughness of the AgNW junction made of two AgNWs (44.5 nm) was decreased similarly to that of a single AgNW (22.2 nm) after the welding (26.3 nm), therefore the surface roughness was significantly reduced by the welding. Because it is easy to increase the induction heating power and the size of the system for the generation of an Eddy current on a large scale, it is believed that this novel welding method can be applied not only to all kinds of M-NWs on various flexible low-temperature polymer substrates but also to a large area at a short time and at low cost.

Acknowledgments

This study was supported by the MOTIE (Ministry of Trade, Industry & Energy) (10048504) and KSRC (Korea Semiconductor Research Consortium) support program for the development of the future semiconductor device. It was also supported by the Nano Material Technology Development Program through the National Research Foundation Korea (NRF), funded by the Ministry of Education, Science, and Technology (2016M3A7B4910429).

ORCID iDs

Geun Young Yeom https://orcid.org/0000-0001-6603-2193

References

[1] Hecht D S, Hu L and Irvin G 2011 Emerging transparent electrodes based on thin films of carbon nanotubes, graphene, and metallic nanostructures *Adv. Mater.* **23** 1482–513

[2] Li N, Oida S, Tulevski G S, Han S-J, Hannon J B, Sadana D K and Chen T-C 2013 Efficient and bright organic light-emitting diodes on single-layer graphene electrodes *Nat. Commun.* **4** 2294

[3] Lipomi D J, Vosgueritchian M, Benjamin C-K T, Hellstrom S L, Lee J A, Fox C H and Bao Z 2011 Skin-like pressure and strain sensors based on transparent elastic films of carbon nanotubes *Nat. Nanotechnol.* **6** 788–92

[4] Cho D-Y, Eun K, Choa S-H and Kim H-K 2014 Highly flexible and stretchable carbon nanotube network electrodes prepared by simple brush painting for cost-effective flexible organic solar cells *Carbon* **66** 530–8

[5] Won S, Hwangbo Y, Lee S-K, Kim K-S, Kim K-S, Lee S-M, Lee H-J, Ahn J-H, Kim J-H and Lee S-B 2014 Double-layer CVD graphene as stretchable transparent electrodes *Nanoscale* **6** 6057–64

[6] Lee M-S *et al* 2013 High-performance, transparent, and stretchable electrodes using graphene−metal nanowire hybrid structures *Nano Lett.* **13** 2814–21

[7] Vosgueritchian M, Lipomi D J and Bao Z 2012 Highly conductive and transparent PEDOT:PSS films with a fluorosurfactant for stretchable and flexible transparent electrodes *Adv. Funct. Mater.* **22** 421–8

[8] Lipomi D J, Lee J A, Vosgueritchian M, Tee B C-K, Bolander J A and Bao Z 2012 Electronic properties of transparent conductive films of PEDOT:PSS on stretchable substrates *Chem. Mater.* **24** 373–82

[9] Nam S *et al* 2014 Ultrasmooth, extremely deformable and shape recoverable Ag nanowire embedded transparent electrode *Sci. Rep.* **4** 4788

[10] Madaria A R, Kumar A, Ishikawa F N and Zhou C 2010 Uniform, highly conductive, and patterned transparent films of a percolating silver nanowire network on rigid and flexible substrates using a dry transfer technique *Nano Res.* **3** 564–73

[11] Gaynor W, Burkhard G F, McGehee M D and Peumans P 2011 Smooth nanowire/polymer composite transparent electrodes *Adv. Mater.* **23** 2905–10

[12] Jeong J and Jeong J 2018 Analysis of plasma treatment effects on a compliant substrate for *Appl. Sci. Converg. Technol.* **27** 5–8

[13] Wang R and Ruan H 2016 Synthesis of copper nanowires and its application to flexible transparent electrode *J. Alloys Compd.* **656** 936–43

[14] Han S *et al* 2014 Fast plasmonic laser nanowelding for a Cu-nanowire percolation network for flexible transparent conductors and stretchable electronics *Adv. Mater.* **26** 5808–14

[15] Won Y, Kim A, Lee D, Yang W, Woo K, Jeong S and Moon J 2014 Annealing-free fabrication of highly oxidation-resistive copper nanowire composite conductors for photovoltaics *NPG Asia Mater.* **6** e105–9

[16] Guo H *et al* 2013 Copper nanowires as fully transparent conductive electrodes *Sci. Rep.* **3** 2323

[17] Nam V B and Lee D 2016 Copper nanowires and their applications for flexible, transparent conducting films: a review *Nanomaterials* **6** 47

[18] Kim T, Canlier A, Kim G H, Choi J, Park M and Han S M 2013 Electrostatic spray deposition of highly transparent silver nanowire electrode on flexible substrate *ACS Appl. Mater. Interfaces* **5** 788–94

[19] Lee J Y, Connor S T, Cui Y and Peumans P 2008 Solution-processed metal nanowire mesh transparent electrodes *Nano Lett.* **8** 689–92

[20] Hwang B, Kim T and Han S M 2016 Compression and tension bending fatigue behavior of Ag nanowire network *Extrem. Mech. Lett.* **8** 266–72

[21] Zhang D, Wang R, Wen M, Weng D, Cui X, Sun J, Li H and Lu Y 2012 Synthesis of ultralong copper nanowires for high-performance transparent electrodes *J. Am. Chem. Soc.* **134** 14283–6

[22] Chu H C, Chang Y C, Lin Y, Chang S H, Chang W C, Li G A and Tuan H Y 2016 Spray-deposited large-area copper nanowire transparent conductive electrodes and their uses for touch screen applications *ACS Appl. Mater. Interfaces* **8** 13009–17

[23] Zhong Z, Lee H, Kang D, Kwon S, Choi Y-M, Kim I, Kim K-Y, Lee Y, Woo K and Moon J 2016 Continuous patterning of copper nanowire-based transparent conducting electrodes for use in flexible electronic applications *ACS Nano* **10** 7847–54

[24] Langley D, Giusti G, Mayousse C, Celle C, Bellet D and Simonato J-P 2013 Flexible transparent conductive materials based on silver nanowire networks: a review *Nanotechnology* **24** 452001

[25] Jin Y, Wang K, Cheng Y, Pei Q, Xu Y and Xiao F 2017 Removable large-area ultrasmooth silver nanowire transparent composite electrode *ACS Appl. Mater. Interfaces* **9** 4733–41

[26] Liu C-H and Yu X 2011 Silver nanowire-based transparent, flexible, and conductive thin film *Nanoscale Res. Lett.* **6** 75

[27] Akter T and Kim W S 2012 Reversibly stretchable transparent conductive coatings of spray-deposited silver nanowires *ACS Appl. Mater. Interfaces* **4** 1855–9

[28] Huang G-W, Xiao H-M and Fu S-Y 2015 Wearable electronics of silver-nanowire/poly(dimethylsiloxane) nanocomposite for smart clothing *Sci. Rep.* **5** 13971

[29] Oh J S, Oh J S, Shin J H, Yeom G Y and Kim K N 2015 Nano-welding of Ag nanowires using rapid thermal annealing for transparent conductive films *J. Nanosci. Nanotechnol.* **15** 8647–51

[30] Sepulveda-Mora S B and Cloutier S G 2012 Figures of merit for high-performance transparent electrodes using dip-coated silver nanowire networks *J. Nanomater.* **2012** 7

[31] Langley D P, Lagrange M, Giusti G, Jiménez C, Bréchet Y, Nguyenb N D and Bellet D 2014 Metallic nanowire networks: effects of thermal annealing on electrical resistance *Nanoscale* **6** 13535

[32] Hauger T C, Al-Rafia S M I and Buriak J M 2013 Rolling silver nanowire electrodes: simultaneously addressing adhesion, roughness, and conductivity *ACS Appl. Mater. Interfaces* **5** 12663–71

[33] Lee S J *et al* 2014 A roll-to-roll welding process for planarized silver nanowire electrodes *Nanoscale* **6** 11828

[34] Tokuno T, Nogi M, Karakawa M, Jiu J, Nge T T, Aso Y and Suganuma K 2011 Fabrication of silver nanowire transparent electrodes at room temperature *Nano Res.* **4** 1215–22

[35] Song T-B, Chen Y, Chung C-H, Yang (Michale) Y, Bob B, Duan H-S, Li G, Tu K-N, Huang Y and Yang Y 2014 Nanoscale Joule heating and electromigraton enhanced ripening of silver nanowire contacts *ACS Nano* **8** 2804–11

[36] Seong B, Chae I, Lee H, Nguyenb V D and Byun D 2015 Spontaneous self-welding of silver nanowire networks *Phys. Chem. Chem. Phys.* **17** 7629

[37] Shiau Y-J, Chiang K-M and Lin H-W 2015 Performance enhancement of metal nanowire-based transparent electrodes by electrically driven nanoscale nucleation of metal oxides *Nanoscale* **7** 12698–705

[38] Garnett E C, Cai W, Cha J J, Mahmood F, Connor S T, Christoforo M G, Cui Y, McGehee M D and Brongersma M L 2012 Self-limited plasmonicwelding of silver nanowire junctions *Nat. Mater.* **11** 241–9

[39] Mallikarjuna K, Hwang H-J, Chunga W-H and Kim H-S 2016 Photonic welding of ultra-long copper nanowire network for flexible transparent electrodes using white flash light sintering *RSC Adv.* **6** 4770

[40] Park J H, Hwang G-T, Kim S, Seo J, Park H-J, Yu K, Kim T-S and Lee K J 2017 Flash-induced self-limited plasmonic welding of silver nanowire network for transparent flexible energy harvester *Adv. Mater.* **29** 1603473

[41] Hu L, Kim H S, Lee J-Y, Peumans P and Cui Y 2010 Scalable coating and properties of transparent, flexible, silver nanowire electrodes *ACS Nano* **4** 2955–63

[42] Xiong W *et al* 2016 Highly conductive, air-stable silver nanowire@Iongel composite films toward flexible transparent electrodes *Adv. Mater.* **28** 7167–72

[43] Ahn J, Seo J-W, Kim J Y, Lee J, Cho C, Kang J, Choi S-Y and Lee J-Y 2016 Self-supplied nano-fusing and transferring metal nanostructures via surface oxide reduction *ACS Appl. Mater. Interfaces* **8** 1112–9

[44] Kang H, Kim Y, Cheon S, Yi G-R and Cho J H 2017 Halide welding for silver nanowire network electrode *ACS Appl. Mater. Interfaces* **9** 30779–85

[45] Zhu R *et al* 2011 Fused silver nanowires with metal oxide nanoparticles and organic polymers for highly transparent conductors *ACS Nano* **5** 9877–82

[46] Lee J, Lee P, Lee H B, Hong S, Lee I, Yeo J, Lee S S, Kim T-S, Lee D and Ko S H 2013 Room-temperature nanosoldering of a very long metal nanowire network by conducting-polymer-assisted joining for a flexible touch-panel application *Adv. Funct. Mater.* **23** 4171–6

[47] Lu H, Zhang D, Cheng J, Liu J, Mao J and Choy W C H 2015 Locally welded silver nano-network transparent electrodes with high operational stability by a simple alcohol-based chemical approach *Adv. Funct. Mater.* **25** 4211–8

[48] Liang J, Li L, Tong K, Ren Z, Hu W, Niu X, Chen Y and Pei Q 2014 Silver nanowire percolation network soldered with graphene oxide at room temperature and its application for fully stretchable polymer light-emitting diodes *ACS Nano* **8** 1590–600

[49] Liu Y, Zhang J, Gao H, Wang Y, Liu Q, Huang S, Guo C F and Ren Z 2017 Capillary-force-induced cold welding in silver-nanowire-based flexible transparent electrodes *Nano Lett.* **17** 1090–6

[50] Chung W-H, Kim S-H and Kim H-S 2016 Welding of silver nanowire networks via flash white light and UV-C irradiation for highly conductive and reliable transparent electrodes *Sci. Rep.* **6** 32086

[51] Rudnev V, Loveless D and Cook R L 2018 *Handbook of Induction Heating* 2nd edn (Boca Raton, FL: CRC Press)

[52] Lucía O, Maussion P, Dede E J and Burdío J M 2014 Induction heating technology and its applications: past developments, current technology, and future challenges *IEEE Trans. Ind. Electron.* **61** 2509–20

[53] Tsuboi H, Ikeda K, Kurata M, Kainuma K and Nakamura R 1998 Eddy current analysis for the pipe welding *IEEE Trans. Magn.* **34** 1234–6

[54] Sosnowchik B D, Azevedo R G, Myers D R, Chan M W, Pisano A P and Lin L 2012 Rapid silicon-to-steel bonding by induction heating for MEMS strain sensors *J. Microelectromechanical Syst.* **21** 497–506

[55] Kurose H, Miyagi D, Takahashi N, Uchida N and Kawanaka K 2009 3D Eddy current analysis of induction heating apparatus considering heat emission, heat conduction, and temperature dependence of magnetic characteristics *IEEE Trans. Magn.* **45** 1847–50

[56] Park K, Eom H and Ik Lee S 2010 Fully-integrated numerical analysis of micro-injection molding with localized induction heating *AIP Conf. Proc.* **1252** 192–7

[57] Chen S C, Jong W R and Chang J A 2006 Dynamic mold surface temperature control using induction heating and its effects on the surface appearance of weld line *J. Appl. Polym. Sci.* **101** 1174–80

[58] Chen Z, Ye S, Stewart I E and Wiley B J 2014 Copper nanowire networks with transparent oxide shells that prevent oxidation without reducing transmittance *ACS Nano* **8** 9673–9

[59] Kholmanov I N, Domingues S H, Chou H, XiaohanW, Tan C, Kim J-Y, Li H, Piner R, Zarbin A J G and Ruoff R S 2013 Reduced graphene oxide/copper nanowire hybrid films as high-performance transparent electrodes *ACS Nano* **7** 1811–6